Revealing Unusual Bonding Situations

Frank R. Wagner, Alexei I. Baranov, Carina Bergner, Viktor Bezugly[1], Yuri Grin, and Miroslav Kohout

In order to be able to generate a firm basis concerning the normal bonding situation and to identify and explore the more exotic ones, a most general and widely applicable set of theoretical instruments has to be at one's disposal. We chose to utilize and develop the analysis of electronic behavior in position space on the basis of reduced density matrices. This way, the methodology developed does not explicitly depend on a specific type of basis set or treatment of electron correlation. It is the common kernel part of all electronic structure methods that is utilized. Thus, the methods of analysis can be employed at any level of electron correlation treatment to molecules and to solids as well.

The presently employed quantities are the electron density and its complete spatial partitioning into atomic regions, i.e., the QTAIM topological atoms, the electron localizability indicator (ELI) in various variants [1], and the electronic localization and delocalization index between spatial regions [2]. The following investigations have been pursued because of their prototypical character for emerging and unusual bonding situations in complex solids.

Our basic understanding of chemical bonding mostly originates from structurally and electronically very simple units, ultimately H_2^{1+} and H_2. Although structurally still simple, in the series of Li_2–Ne_2 each molecule displays a prototypical bonding situation on its own, and often an adequate theoretical treatment has to take electron correlation into account explicitly. A systematic investigation of the behavior of ELI-D and singlet-ELI at a highly correlated level of theory was undertaken in order to a) obtain a reliable representation of ELI for these complex bonding situations, and b) analyze the effects of electron correlation on the position-space chemical bonding descriptors used [3].

Although Li_2 is isoelectronic to H_2 and the formal bond order according to Herzberg is 1, the bond is significantly weaker due to the influence of the filled 1st atomic shell. This influence manifests itself in the valence region of the ELI-D distribution as a specific structuring yielding either one (bond attractor) or three (one bond and two atomic attractors) ring attractors depending on the amount of electron correlation included. At sufficiently high level only the ring attractor in the bonding region remains, where the absence of the point attractor is caused by the closed-shell interaction between the first atomic shells of Li.

Be_2 is a molecule built from two closed shell atoms isoelectronic to He, and the formal bond order is therefore zero. The attraction between the atoms mostly results from electron correlation. Still, the bond is an order of magnitude stronger than those caused from dispersion forces in Ne_2. The ELI-D displays a split-attractor scenario at the bond midpoint and two bond-opposed lone pair regions, which is consistent with the picture of a weak, shared interaction of an intrinsically stretched bond. Noteworthy, this topology is already found at the HF level of theory, where the molecule is not stable.

B_2 is an open-shell triplet molecule because it prefers two π half-bonds (i.e., half-filled pπ bonding orbitals) instead of a single σ bond (i.e., completely filled pσ orbital), which is a correlation effect. With the formal bond order of one, it represents an exotic single bond resulting from π bonding alone. The ELI-D distribution for the minority spin channel resembles the one for Be_2, however with a non-split attractor at the bond midpoint. On the other hand, the ELI-D for the majority spin channel yields two ring attractors around each of the atoms, but no bond attractor. This is observed at all levels of theory investigated. The combined ELI-D diagram can be obtained by calculating the variant for triplet-coupled electron pairs, called triplet-ELI-D [1]. While HF displays no bond attractor of triplet-ELI-D at all, all the methods considering electron correlation yield a ring attractor at the bond midpoint resulting from the π bonding interaction and two bond-opposed lone-pair attractors inherited from the Be_2 scenario.

With two electrons more than B_2 which fill up the two open shell π orbitals, the closed-shell molecule C_2 displays an exotic type of formal double bond with two pπ bonds accompanied by the σ/σ^* com-

bination, as in Be_2. The effective non-cancellation of the σ bonding by the σ/σ* combination yields, similar to Be_2, an additional σ bonding contribution not taken into account in the formal bond order evaluation. Therefore, the C–C distance is markedly shorter than for the usual σπ-bonding situation in e.g., C_2H_4. For this molecule the ELI-D topology was the most difficult to converge with respect to electron correlation treatment. Finally, a ring attractor at the bond midpoint and two atomic ring attractors are displayed. The ELI-D topology is to be interpreted as a type of strongly split, ring-shaped bond attractor owing to the π character.

The only truly classical covalent molecule of the series appears with N_2, which represents the prototype example of a triple bond. All methods yield the same topology of ELI-D, namely a point attractor at the bond midpoint and two lone pair attractors at the bond-opposed sides.

Another example of a formal double bond is realized for O_2, but this is achieved with an open-shell triplet wavefunction. The half-occupation of the π* orbitals and the remaining pσ bond makes it a σπ double bond – in contrast to C_2 with a ππ' one. The minority- and majority-spin resolved ELI-D diagrams roughly resemble the corresponding ones for the isoelectronic molecules N_2 and F_2, respectively. The topology of triplet-ELI-D is found to be the same as that for the majority spin component with a point attractor at the bond midpoint and two atomic ring attractors.

Molecule F_2 formally displays a single bond which is known to be rather weak. From the analysis of VB wavefunctions characteristically large ionic contributions have been found which make F_2 a prototype example for charge-shift bonding. The stretched-bond scenario is indicated in the ELI-D topology by a split bond-attractor scenario which occurs at all correlated levels of theory. The lone-pair region is indicated by an atomic ring attractor for each atom.

The Ne_2 unit with formal bond order of zero represents an example for van der Waals bonding. The optimized interatomic distance of 295 pm at CI-SD level is found to be rather close to the experimental one (291 pm). The ELI-D topology for all types of calculations employing this interatomic distance yields no bond attractor but a deep (3, –1) saddle point instead. This finding is consistent with the notion that van der Waals bonding does not lead to localizable single electrons in the "bonding region".

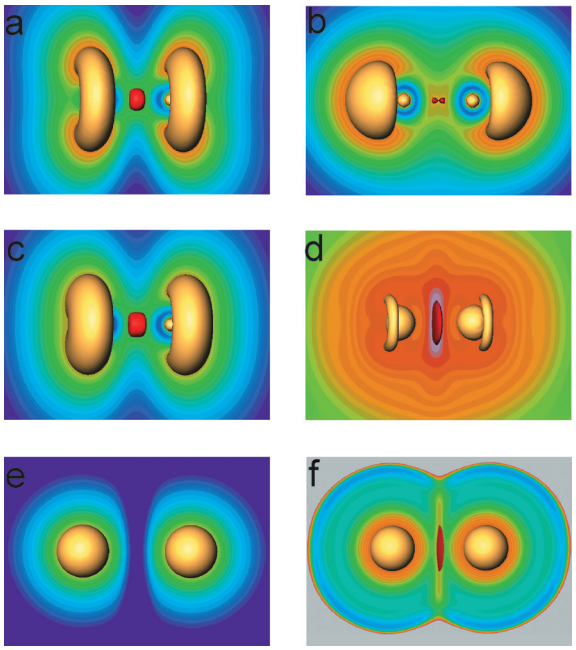

Fig. 1: O_2 (a-d) and Ne_2 (e, f): ELI-D for (a, e) majority and (b) minority spin channel, (c) triplet-pair ; (d, f) ELIA.

The localizability of opposite-spin electron pairs has also been investigated by the related quantities ELIA and singlet-ELI-q [1]. It can be sensibly calculated only for explicitly correlated pair densities because it adopts a constant value of 1 everywhere in space for monodeterminantal wavefunctions as used in HF or Kohn-Sham DFT methods. For the molecules Li_2–F_2 a region of locally increased localizability of opposite-spin electron pairs (from ELIA) between the atoms is found in parallel to the increased single electron localizability described by ELI-D (e.g., O_2, Fig 1a-d). It is quite striking that for Ne_2 this is not the case. Here the single-electron localizability is found to decrease along the internuclear line up to the midpoint, accompanied by an increasing pairing of opposite-spin electrons which leads to a local maximum of opposite-spin electron pair localizability (ELIA) at the "bond midpoint" (Fig. 1e, f), similar to Li_2–F_2. This clearly indicates that the low localizability of an α-spin electron and a β-spin electron in the same volume element does not automatically lead to low αβ-pair localizability. Concerning the notion of van der Waals bonding, even for this case of avoided electron sharing between the atoms a local opposite-spin pairing is found, similar to typical chemical bonds.

Metal–metal bonding involving transition metals is a fascinating topic for experimentalists and theoreticians alike [4]. Of special interest are those situations in which the metal atoms are not interlinked by a common ligand. Typically, these situations can be found for molecular compounds but are scarce for collective solids. They represent prototypical situations for studies of metal–metal bonding which yield important basic information that can be used to better understand more complex metal–metal bonding situations in solids.

In 2008 our cooperation partner within the SPP1166, Prof. Rhett Kempe (Univ. Bayreuth) and his group, succeeded to synthesize and structurally characterize a class of compounds displaying the very rare situation of a short, unsupported *TM–RE* contact, Cp_2Re–*RE*Cp_2 (*RE*=Y, Yb) [5] with *d*(Re–Y) = 296 pm. The chemical bonding analysis of the Y compound (1) [5] on the basis of the topological analysis of the calculated (DFT/BLYP method) electron density and ELI-D yields three ELI-D basins in the valence shell of Re. While two of them can be considered to represent lone-pair-type regions, a disynaptic (i.e., bond-indicating) basin between Re and *RE* is found, whose attractor lies within the QTAIM Re atom, and whose electronic population belongs to 84% to that atom. This conforms to the picture of a rather polar covalent bond *TM–RE*. As a 'Gedankenexperiment' the bond can be heterolytically dissected resulting in the fragments $[Cp_2Re]^-$ (isoelectronic to $FeCp_2$, fulfills the 18e rule) and $[RECp_2]^+$. Calculation of ELI-D for the separate fragments yields for $[Cp_2Re]^-$ a Re lone pair pointing in the direction of the *RE* atom in the $[RECp_2]^+$ fragment, where the latter one displays a region of low electron localizability. The observation of compatible regions of electron localizability along with the fact that the orbital, which is responsible for the Re lone pair (from pELI-D orbital decomposition [1]), is the HOMO of the $[Cp_2Re]^-$ fragment, points toward the notion of a dative bond $(Re^{1+}\rightarrow)RE^{3+}$ involving a transition metal lone pair at a formal Re^{1+} species.

$[\{(CO)_2CpRu\}_2Yb(tBu\text{-}py)_3]$ (**2**) and $[\{Cp_2Re\}_2Yb(thf)_2]$ (**3**) are the first molecular examples containing unsupported $TM–RE^{2+}$ bonds [6]. The bonding analysis of **2** reveals one disynaptic ELI-D basin per Ru–Yb contact. For compound **3** two disynaptic ELI-D basins are found for each Re–Yb contact, which is a consequence of the edge-on orientation of the Cp ring at each $ReCp_2$ fragment with respect to the Re–*RE* bond axis direction. For Cp_2Re–$LaCp^*_2$ (**4**) the same effect is found. The two combined basins possess the same population as the disynaptic one discussed for **1,** and the intersection by the QTAIM atoms again yields very similar values as in **1** and **2**. The effective charge found for each $[ReCp_2]$ and $[(CO)_2CpRu]$ fragment in **2** and **3** is 0.7– in all cases, which is consistently slightly lower in magnitude than the common formal charge of 1–. Moreover, the different formal charges of the Re^{1+} and Ru^0 species are reflected in a graduation of the effective charges of the corresponding QTAIM atoms according to $Re^{0.68+}$ and $Ru^{0.44+}$.

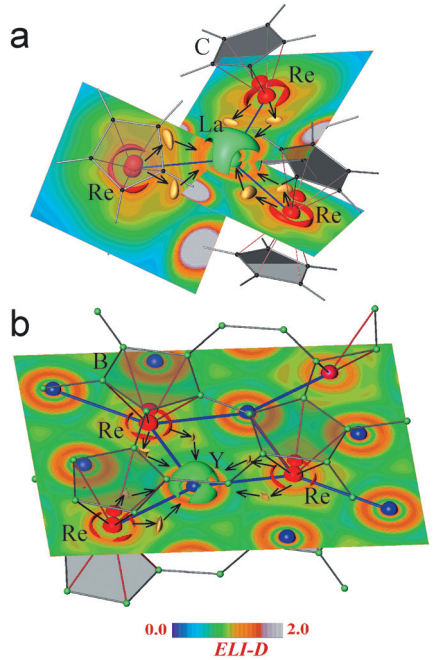

Fig. 2: ELI-D distribution for (a) the $LaRe_3$ core of **5**; (b) the YRe_3 unit of Y_2ReB_6. The green and red coloured isosurfaces visualize the structure of the penultimate shells of *RE* and Re atoms, respectively. The yellow isosurfaces reveal the maxima of ELI-D reflecting the *RE*–Re bonds. The arrows serve as a guide to the eye to emphasize the ELI-D bond attractor scenario.

The molecular structure of the tetrametallic compounds $[RE\{ReCp_2\}_3]$ (*RE* = La, Sm, Lu) (**5**) exhibits a slightly distorted trigonal planar coordination of *RE* by Re (e.g., *d*(La–Re) = 305 pm on average) (Fig. 2a). The *RE* atom is solely coordinated by three Re metal atoms, a coordination motif which is without precedence for a stable molecule in *RE* chemistry. The position-space bonding analysis revealed two disynaptic ELI-D basins per

La–Re contact [7] similar to **3** and **4**. Thus, the compounds can be formulated to contain a $[(Re^{1+}\rightarrow)_3RE^{3+}]$ metallic core. An interaction energy (averaged over three possibilities) of –527(±5) kJ mol^{-1} between one $[Cp_2Re]^{1-}$ fragment (unrelaxed) and the remaining $\{RE\{ReCp_2\}_2\}^{1+}$ fragment has been calculated within the framework of the Morokuma-Ziegler energy decomposition analysis. A dominant electrostatic energy contribution of 68% is found, which is not surprising taking into account the charged nature of the fragments. The sizable orbital interaction, which provides the remaining 32% energy contribution, is fully consistent with the bonding scenario extracted from the ELI-D and QTAIM analysis. Moreover, although the fragments are oppositely charged, the *TM* and *RE* atoms are both positively charged (QTAIM effective charges) such that an electrostatic attraction is ruled out as an explanation of the *TM–RE* bonding.

The occurrence of a purely metallic core in **5** suggests a comparison with the intermetallic compounds. In binary *RE-TM* phases a triangular arrangement of the *TM* atoms around the *RE* atoms is often found, however only as a part of the coordination sphere of the *RE* (e.g., in $PrRe_2$ with $MgZn_2$ structure type). This is caused by the fact that there is no structural unit playing the shielding role of Cp in **5**. Allowing for a third component, which can play this role, one finds a highly related situation in Y_2ReB_6. The B atoms form (A, A) stacks of planar layers of 5-, 6-, and 7-membered rings between which the metal atoms are sandwiched. The Re atoms are always sandwiched between 5-membered rings, Y1 atoms between 6- and Y2 between 7-membered rings. The sandwiched situation of the Re atoms is very similar to **5**, but with the rings now all being coplanar. Similar as *RE* in **5**, the Y2 atoms display three Re neighbors within the metal plane, however at slightly larger distances of 308 pm (2 ×) and 320 pm (1 ×). The striking observations in the calculated ELI-D distributions are: i) the Re atoms display the same kind of structuring of the penultimate shell and ii) the occurrence of the same pattern of ELI-D maxima in the valence shell for the Re–Y bonding situation. Together, this indicates a similar type of Re–Lu bonding. From this point of view the novel compounds **5** represent the missing link in the conceptual evolution from *RE–TM* organometallic coordination compounds to intermetallic compounds [7].

In summary, the *TM–RE* bonding in the intermetallic phase Y_2ReB_6 can be traced back to $[(Cp_2Re)_3RE]$, and further to $[(Cp_2Re)RECp_2]$, with all of them showing polar, dative (Re→)*RE* type of bonding. But the implications of this finding go much further. In solid state compounds with low-valent transition metals as nitridometalates, carbometalates [8], cyanidometalates [9], metallogallates [10], and phosphidometalates [11], which are the subject of various studies in our institute, related chemical bonding situations have been detected. This establishes the actual relevance behind the introductory remark that these molecular compounds display prototypical bonding situations for the more complex metal–metal bonding in solids.

References

[1] *Miroslav Kohout, Frank R. Wagner, Alexei I. Baranov, Carina Bergner, Viktor Bezugly, and Kati Wagner*, in Scientific Report 2006-2008, p. 65 (Max Planck Institute for Chemical Physics of Solids, Dresden Germany, 2009)

[2] *M. Kohout, Alexei I. Baranov, Kati Finzel, and Frank R. Wagner*, in Scientific Report 2009-2010, 127 (Max Planck Institute for Chemical Physics of Solids, Dresden Germany, 2011)

[3] a) *V. Bezugly, P. Wielgus, M. Kohout, and F. R. Wagner*, J. Comput. Chem. **31** (2010) 1504; b) *ibid*., J. Comput. Chem. **31** (2010) 2273.

[4] *F. R. Wagner and A. Noor, and R. Kempe,* Nature Chem. **1** (2009) 529.

[5] *M. V. Butovskii, O.L. Tok, F. R. Wagner, and R. Kempe*, Angew. Chem. Int. Ed. **47** (2008) 6469.

[6] *C. Döring, A. Dietel, M. V. Butovskii, V. Bezugly, F. R. Wagner, and R. Kempe*, Chem. Eur. J, **16** (2010) 10679.

[7] *M. V. Butovskii, C. Döring, V. Bezugly, F. R. Wagner, and R. Kempe*, Nature Chem. **2** (2010) 741.

[8] a) *E. Dashjav, Y. Prots, G. Kreiner, W. Schnelle, F. R. Wagner, and R. Kniep*, J. Solid State Chem. **181** (2008), 3121; b) *B. Davaasuren, H. Borrmann, E. Dashjav, G. Kreiner, M. Widom, W. Schnelle, F. R. Wagner, and R. Kniep*, Angew. Chem. Int. Ed. **48** (2010), 5688.

[9] *Peter Höhn et al.*, in Scientific Report 2009-2010, 66 (Max Planck Institute for Chemical Physics of Solids, Dresden Germany, 2011)

[10] *O. S. Sichevich, M. Kohout, W. Schnelle, H. Borrmann, R. Cardoso-Gil, M. Schmidt, U. Burkhard, and Yu. Grin*, Inorg. Chem. **48** (2009) 6261.

[11] *P. S. Chizhov, Y. Prots, E. V. Antipov, and Yu. Grin*, Z. Anorg. Allg. Chem. **635** (2009) 1863.

[1] Present address: Institut für Werkstoffwissenschaft, Techn. Universität Dresden, 01062 Dresden, Germany